Received 2013 October 29; accepted 2014 May 27; published 2014 June 23
Preprint typeset using LaTeX style emulateapj v. 5/2/11

arXiv:1405.7097v2 [astro-ph.HE] 25 Jun 2014

EPISODIC JET POWER EXTRACTED FROM A SPINNING BLACK HOLE SURROUNDED BY A NEUTRINO-DOMINATED ACCRETION FLOW IN GAMMA-RAY BURSTS

Xinwu Cao[1,2], En-Wei Liang[3], and Ye-Fei Yuan[4]

Received 2013 October 29; accepted 2014 May 27; published 2014 June 23

ABSTRACT

It was suggested that the relativistic jets in gamma-ray bursts (GRBs) are powered via the Blandford-Znajek (BZ) mechanism or the annihilation of neutrinos and anti-neutrinos from a neutrino cooling-dominated accretion flow (NDAF). The advection and diffusion of the large-scale magnetic field of a NDAF is calculated, and the external magnetic field is found to be dragged inward efficiently by the accretion flow for a typical magnetic Prandtl number $\mathscr{P}_{\rm m}=\eta/\nu\sim 1$. The maximal BZ jet power can be $\sim 10^{53}-10^{54}$ erg s^{-1} for an extreme Kerr black hole, if an external magnetic field with 10^{14} Gauss is advected by the NDAF. This is roughly consistent with the field strength of the disk formed after a tidal disrupted magnetar. The accretion flow near the black hole horizon is arrested by the magnetic field if the accretion rate is below than a critical value for a given external field. The arrested accretion flow fails to drag the field inward and the field strength decays, and then the accretion re-starts, which leads to oscillating accretion. The typical timescale of such episodic accretion is in an order of one second. This can qualitatively explain the observed oscillation in the soft extend emission of short-type GRBs.

Subject headings: accretion, accretion disks, black hole physics, gamma-ray burst: general

1. INTRODUCTION

It is believed that gamma-ray bursts (GRBs) are powered by the accretion disks surrounding stellar-mass black holes (Popham et al. 1999; Narayan et al. 2001). The observed high luminosity of GRBs requires a very large mass accretion rate, $\dot{M}\sim 0.01-10\ M_{\odot}{\rm s}^{-1}$, and therefore the accretion disks are massive with mass of $0.1-1\ M_{\odot}$. The gas in the accretion disks is so dense that the most photons emitted in the disks cannot escape the systems, which leads to high temperature of the disks, $\gtrsim 10^{10}$ K. Thus, the neutrino cooling becomes dominant over the photon radiation, and therefore the accretion disks are named as "neutrino-dominated accretion flows" (NDAF, Popham et al. 1999; Narayan et al. 2001; Di Matteo et al. 2002; Kohri & Mineshige 2002; Kohri et al. 2005; Gu et al. 2006; Chen & Beloborodov 2007; Kawanaka & Mineshige 2007; Liu et al. 2007; Pan & Yuan 2012) .

The widely discussed jet formation mechanisms for GRBs are the Blandford-Znajek (BZ) mechanism or the annihilation of neutrinos and anti-neutrinos from an NDAF (e.g., Popham et al. 1999; Li 2000; Narayan et al. 2001; Di Matteo et al. 2002; Kohri & Mineshige 2002; Wang et al. 2002; McKinney 2005; Lee et al. 2005; Gu et al. 2006; Chen & Beloborodov 2007; Janiuk et al. 2008; Lei et al. 2009; Liu et al. 2012). Based on lack of detection of a thermal photosphere component predicted by the baryonic fireball model in the GRB spectra observed with the *Fermi* mission (e.g., Abdo et al. 2009; Zhang et al. 2011), it was proposed that the GRB jet would be highly magnetized (e.g., Zhang & Peer 2009; Zhang & Yan 2011; see also Daigne & Mochkovitch 2002; Zhang & Meszaros 2002). More recently, Yuan & Zhang (2012) proposed a new model for the jet formation in GRBs. The episodic, magnetically dominated plasma blobs are suggested to be ejected from the corona of a hyper accretion disk, which are responsible for the observed episodic prompt gamma-ray emission from GRBs, as suggested by Zhang & Yan (2011).

The most extensively discussed mechanism for powering a magnetized jet is the BZ mechanism (Blandford & Znajek 1977), in which the energy and angular momentum are extracted from a rotating black hole with the large scale magnetic field lines. The power of the jet launched by a rotating black hole surrounded by a NDAF can be estimated when the strength of the magnetic field near the black hole horizon is available. Kawanaka et al. (2013) calculated the BZ power of the jet in GRBs, and found that the typical jet power can be as high as $\sim 10^{53}$ erg s^{-1} assuming the poloidal field to be equipartition with the gas pressure in the inner disk region. In their work, the detailed physics of the large scale field formation has not been considered.

A NDAF is probably formed after a merger of black hole/neutron binary (e.g., Eichler et al. 1989; Ruffert & Janka 1998; Barkov & Komissarov 2010; Etienne et al. 2012; Deaton et al. 2013; Foucart et al. 2013) or the gravitational collapse of a massive star (e.g., Woosley 1993; Paczynski 1998; Piran 2004; Zhang & Mészáros 2004; Woosley & Bloom 2006). In the merger scenario, a disk is formed to feed the black hole after a neutron star is tidally disrupted, and the

[1] Key Laboratory for Research in Galaxies and Cosmology, Shanghai Astronomical Observatory, Chinese Academy of Sciences, 80 Nandan Road, Shanghai, 200030, China; cxw@shao.ac.cn
[2] Department of Astronomy and Institute of Theoretical Physics and Astrophysics, Xiamen University, Xiamen, Fujian, 361005, China
[3] Department of Physics and GXU-NAOC Center for Astrophysics and Space Sciences, Guangxi University, Nanning, 530004, China; lew@gxu.edu.cn
[4] Department of Astronomy, University of Sciences and Technology of China, Hefei, Anhui, 230026, China; yfyuan@ustc.edu.cn

strong magnetic field may be formed near the black hole with an external field dragged inward by the NDAF. The NDAF is driven by turbulence, which also makes the field diffuse outwards. A steady magnetic field configuration of the disk is available when the advection is balanced with the diffusion of the field in the disk (Lubow et al. 1994).

The diffusivity η of the magnetic field is closely related to the viscosity ν. The magnetic diffusivity should be at the same order of the viscosity in isotropic turbulent fluid, i.e., $\mathscr{P}_{\rm m}=\eta/\nu\sim 1$ (Parker 1979). This is indeed conformed by many different numerical simulations (e.g., Yousef et al. 2003; Lesur & Longaretti 2009; Fromang & Stone 2009; Guan & Gammie 2009). The diffusion/advection balance of the large scale magnetic field in the accretion disks has been explored in some previous works (Lubow et al. 1994; Lovelace et al. 2009; Cao 2011; Beckwith et al. 2009; Guilet & Ogilvie 2012, 2013; Cao & Spruit 2013). The advection of the field is found to be efficient for ADAFs (Cao 2011), due to their relative high radial velocities (Narayan & Yi 1994), while it is inefficient for the geometrically thin standard accretion disks (Lubow et al. 1994), unless the thin disks are dominantly driven by the outflows rather than the turbulence (Cao & Spruit 2013).

In this work, we calculate the magnetic field advection/diffusion in a NDAF, and then estimate the maximal jet power can be extracted from a rapidly rotating black hole in GRBs. We describe the model in Section 2, and Sections 3 and 4 contain the results and discussion.

2. MODEL

We assume a vertical and homogeneous external magnetic field to be radially advected by the gas in the NDAF. The global solution of a steady NDAF is available by solving a set of differential equations, namely, the radial and azimuthal momentum equations, the continuity equation, and the energy equation. The energy equation is rather complicated for a NDAF (see, e.g., Popham et al. 1999; Narayan et al. 2001; Di Matteo et al. 2002; Kohri & Mineshige 2002; Kohri et al. 2005; Gu et al. 2006; Chen & Beloborodov 2007; Kawanaka & Mineshige 2007; Liu et al. 2007). Both the photodisintegration cooling and neutrino cooling are included, which are functions of mass accretion rate. The magnetic field advection/diffusion is predominantly determined by the radial velocity of the accretion flow. Similar to the ADAF case, the dynamics of the NDAF are also altered in the presence of the large-scale field, especially in the inner region of the flow, which is properly considered in our calculations. In the following two sub-sections, we briefly summarize the calculations of the structure of a NDAF and its magnetic field configuration.

2.1. *Structure of the NDAF*

The dynamics of a steady NDAF with a large-scale magnetic field can be derived by solving the following differential equations.

The continuity equation is

$$\frac{d}{dR}(\rho R H v_R)=0, \tag{1}$$

which reduces to $-2\pi R\Sigma v_R=\dot{M}$ if the winds from the NDAF are neglected, $\Sigma=2H\rho$, and $\dot{M}$ is the mass accretion rate of the NDAF.

The radial momentum equation is

$$v_R\frac{dv_R}{dR}=-(\Omega_{\rm K}^2-\Omega^2)R-\frac{1}{\rho}\frac{d}{dR}(\rho c_{\rm s}^2)+\frac{B_R^{\rm S}B_z}{2\pi\Sigma}-\frac{B_zH}{2\pi\Sigma}\frac{\partial B_z}{\partial R}, \tag{2}$$

where the pseudo-Newtonian potential is used to simulate the black hole gravity (Paczyńsky & Wiita 1980), $B_R^{\rm S}$ is the radial magnetic field strength at the disk surface $z=\pm H$. The Keplerian angular velocity is $\Omega_{\rm K}^2(R)=GM_{\rm bh}/(R-R_{\rm S})^2R$, and $R_{\rm S}=2GM_{\rm bh}/c^2$.

As suggested by Balbus & Hawley (1991), the radial magnetic fields are sheared into azimuthal fields by the differential rotation of the accretion flow, which triggers magnetorotational instability (MRI) and the MRI-driven turbulence (Balbus & Hawley 1998). In this case, the viscosity can still be approximated as the conventional α-viscosity, though the values of α are somewhat diverse, as shown in the numerical simulations. It is found that the final results of the field advection in the disks are almost independent of the value of α (see Lubow et al. 1994; Cao 2011, for the discussion). The angular momentum equation reads

$$\frac{d\Omega}{dR}=\frac{v_R(j-j_{\rm in})}{\nu R^2}, \tag{3}$$

where j is the specific angular momentum of the accretion flow, and $j_{\rm in}$ is the specific angular momentum of the gas accreted by the black hole. The conventional α-viscosity $\nu=\alpha c_{\rm s}H$ is adopted in our calculations.

The energy equation is

$$\Sigma v_R T\frac{ds}{dR}=Q^+-Q^-, \tag{4}$$

where T and s are the temperature and entropy of the gas, the cooling rate $Q^-=Q_{\rm ph}^-+Q_\nu^-$ ($Q_{\rm ph}^-$ and Q_ν^- are the cooling rates due to photodisintegration and neutrino processes, respectively). Compared with these two terms, the radiation cooling is always much smaller (e.g., Xue et al. 2013), and it is therefore neglected in our calculations. The neutrino cooling rate is

$$Q_\nu^-=\sum_i\frac{2(7/8)\sigma T^4}{(3/4)[\tau_{\nu_i}/2+1/\sqrt{3}+1/(3\tau_{{\rm a},\nu_i})]}, \tag{5}$$

where $\tau_{\nu_i}=\tau_{{\rm s},\nu_i}+\tau_{{\rm a},\nu_i}$ is the sum of the optical depth due to scattering and absorption for each neutrino flavor "i" in the vertical direction. They are functions of ρ, T, and H (see Di Matteo et al. 2002, for the details). The photodisintegration cooling is (Di Matteo et al. 2002)

$$Q_{\rm ph}^-\simeq 10^{29}\rho_{10}v_R\frac{dX_{\rm nuc}}{dR}2H\ \ {\rm ergs\ cm^{-2}\ s^{-1}}, \tag{6}$$

where $\rho_{10}=\rho/10^{10}$ g cm^{-3}, and the mass fraction $X_{\rm nuc}$ of free nucleons is approximately given by

$$X_{\rm nuc}\simeq 34.8\rho_{11}^{-3/4}T_{11}^{9/8}\exp(-0.61/T_{11}). \tag{7}$$

Here $T_{11}=T/10^{11}$ K.

A set of equations described above are closed with an additional equation, i.e., the equation of state

(Popham et al. 1999),

$$p = \frac{1+3X_{\rm nuc}}{4}\rho RT + \frac{11}{12}aT^4 + K\left(\frac{\rho}{\mu_{\rm e}}\right)^{4/3}, \quad (8)$$

where $K = (2\pi hc/3)(3/8\pi m_{\rm n})^{4/3} = 1.24\times10^{15}$ ($m_{\rm n}$ is the nucleon mass), and $\mu_{\rm e}$ is the mass per electron ($\mu_{\rm e} = 2$ is adopted as the previous works). The three terms in Equation (8) are contributed by gas pressure, pressure due to radiation and relativistic electron-positron pairs, and degeneracy pressure from relativistic electrons, respectively. The corresponding expression for the internal energy is

$$u = \frac{1}{\gamma_{\rm gas}-1}\frac{1+3X_{\rm nuc}}{4}RT + \frac{11}{4}\frac{aT^4}{\rho} + 3K\left(\frac{\rho}{\mu_{\rm e}}\right)^{1/3}, \quad (9)$$

where $\gamma_{\rm gas}$ is the ratio of specific heats for baryonic gas. The baryonic gas in NDAFs is non-relativistic, $\gamma_{\rm gas} \simeq 5/3$. The internal energy can be related to pressure as

$$u = \frac{1}{\gamma-1}\frac{p}{\rho}, \quad (10)$$

for two extreme cases, i.e., baryonic gas dominant ($\gamma \simeq 5/3$) or the pressure from relativistic particles and radiation dominant ($\gamma \simeq 4/3$). It is found that the baryonic gas pressure is dominant in a NDAF for a wide mass accretion rate range (Kawanaka et al. 2013). For simplicity, we adopt $\gamma = 5/3$ in calculating the structure of the NDAF. Thus, Equation (4) can be re-written as

$$\frac{2}{(\gamma-1)c_{\rm s}}\frac{dc_{\rm s}}{dR} = -\frac{1}{R} - \frac{1}{H}\frac{dH}{dR} - \frac{1}{v_R}\frac{dv_R}{dR} + \frac{v_R}{\alpha c_{\rm s}^3 R^2 H}(j-j_{\rm in})^2 + \frac{2\pi RQ^-}{\dot{M}c_{\rm s}^2}, \quad (11)$$

in which the continuity equation (1) is substituted. The final results on the advection of the fields in the NDAFs are found to be insensitive to the value of γ adopted.

The accretion flow is vertically compressed by the strong large-scale magnetic fields (Cao & Spruit 2002; Cao 2011). Assuming the pressure gradient to be in equilibrium with gravity in the vertical direction of the accretion flow, the vertical structure of the disk can be described by

$$\frac{dp(z)}{dz} = -\rho(z)\Omega_{\rm K}^2 z - \frac{B_R}{4\pi}\frac{\partial B_R}{\partial z} + \frac{B_R}{4\pi}\frac{\partial B_z}{\partial R}, \quad (12)$$

if the magnetic field line shape in the disk is known (Cao 2011). In principle, the shape of the field line is available by solving the radial and vertical momentum equations of the disk with suitable boundary conditions (see Cao & Spruit 2002, for the detailed discussion), which is too complicated for our present work. To avoid this complexity, we only consider the simplest case assuming the sound speed $c_{\rm s}$ to be constant in the vertical direction of the accretion flow, i.e., $dp/dz = c_{\rm s}^2 d\rho/dz$. In this case, an approximate analytical expression for the field line shape:

$$R - R_{\rm i} = \frac{H}{\kappa_0\eta_{\rm i}^2}(1-\eta_{\rm i}^2+\eta_{\rm i}^2 z^2 H^{-2})^{1/2} - \frac{H}{\kappa_0\eta_{\rm i}^2}(1-\eta_{\rm i}^2)^{1/2}, \quad (13)$$

is proposed, where H is the scale height of the disk [defined as $\rho(H) = \rho(0)\exp(-1/2)$], the field line inclination $\kappa_0 = B_z/B_R^{\rm S}$ at $z = H$, and $\eta_{\rm i} = \tanh(1)$ (Cao & Spruit 2002). The main features of the Kippenhahn-Schlüter model (Kippenhahn & Schlüter 1957) can be well reproduced by this expression either for weak or strong field cases. The disk scale height H can therefore be derived numerically with the magnetic field line shape (13). We adopt a fitting formula suggested by Cao (2011) to calculate the disk scale height in this work,

$$\frac{H}{R} = \frac{1}{2}\left(\frac{4c_{\rm s}^2}{R^2\Omega_{\rm K}^2} + {f_{\rm h}}^2\right)^{1/2} - \frac{1}{2}f_{\rm h}, \quad (14)$$

where

$$f_{\rm h} = \frac{1}{2(1-{\rm e}^{-1/2})\kappa_0}\left(\frac{B_z^2}{4\pi\rho RH\Omega_{\rm K}^2\kappa_0} + \frac{\xi_{\rm bz}B_z^2}{4\pi\rho R^2\Omega_{\rm K}^2}\right), \quad (15)$$

and $\xi_{\rm bz}$ is defined as

$$\frac{\partial B_z}{\partial R} = -\xi_{\rm bz}(R)\frac{B_z}{R}, \quad (16)$$

which is to be calculated as described in Section 2.2. This fitting formula can reproduce the numerical results quite well (Cao & Spruit 2002; Cao 2011). It reduces to $H = c_{\rm s}/\Omega_{\rm K}$ in the absence of magnetic field.

2.2. *Magnetic field configuration of the NDAF*

The induction equation of large-scale (poloidal) magnetic fields is

$$\frac{\partial}{\partial t}[R\psi(R,0)] = -v_R\frac{\partial}{\partial R}[R\psi(R,0)] - \frac{4\pi\eta}{c}\frac{R}{2H}\int_{-H}^{H} J_\phi(R,z_{\rm h})dz_{\rm h}, \quad (17)$$

where $\psi(R,z)$ is the azimuthal magnetic potential, $J_\phi(R,z_{\rm h})$ is the current density at $z = z_{\rm h}$ above/below the mid-plane of the disk (see Cao 2011, for the detailed discussion). The magnetic field potential $\psi(R,z) = \psi_{\rm d}(R,z) + \psi_\infty(R)$ (Lubow et al. 1994). $\psi_{\rm d}(R,z)$ is contributed by the currents in the accretion flow, while $\psi_\infty(R) = B_{\rm ext}R/2$ is the external imposed homogeneous vertical field (see Lubow et al. 1994, for the details). Assuming the azimuthal current to be distributed homogeneously in z-direction, we have

$$J_\phi(R,z_{\rm h}) = \frac{J_\phi^{\rm s}(R)}{2H}, \quad (18)$$

where $J_\phi^{\rm s}(R)$ is the surface current density. The potential $\psi_{\rm d}$ is related to $J_\phi^{\rm s}(R)$ with

$$\psi_{\rm d}(R,z) = \frac{1}{c}\int_{R_{\rm in}}^{R_{\rm out}} R'{\rm d}R' \int_0^{2\pi}\cos\phi'{\rm d}\phi' \times \int_{-H}^{H}\frac{J_\phi(R',z_{\rm h})}{[R'^2+R^2+(z-z_{\rm h})^2-2RR'\cos\phi']^{1/2}}{\rm d}z_{\rm h}.$$

$$= \frac{1}{2Hc}\int_{R_{\rm in}}^{R_{\rm out}} J_\phi^{\rm s}(R')R'{\rm d}R'\int_0^{2\pi}\cos\phi'{\rm d}\phi'$$

$$\times\int_{-H}^{H}\frac{1}{[R'^2+R^2+(z-z_{\rm h})^2-2RR'\cos\phi']^{1/2}}{\rm d}z_{\rm h}. \quad (19)$$

Equation (17) reduces to

$$-\frac{\partial}{\partial R}[R\psi_{\rm d}(R,0)]-\frac{2\pi}{c}\frac{\alpha c_{\rm s}R}{v_R}\mathscr{P}_{\rm m}J_\phi^{\rm S}(R)=B_0R, \quad (20)$$

for steady case, where $\mathscr{P}_{\rm m}=\eta/\nu$. This integro-differential equation can be solved numerically to derive the R-dependent surface current density $J_\phi^{\rm s}(R)$ with the specified $\mathscr{P}_{\rm m}$ if the structure of the NDAF is known (see Lubow et al. 1994, for the details). The configuration of the large-scale magnetic fields can be calculated with the derived potential ψ:

$$B_R(R,z)=-\frac{\partial}{\partial z}\psi(R,z), \quad (21)$$

and

$$B_z(R,z)=\frac{1}{R}\frac{\partial}{\partial R}[R\psi(R,z)]. \quad (22)$$

2.3. *Maximal power of jets in GRBs*

Considering the horizon of a rotating black hole to be threaded by a large scale magnetic field, the rotating energy of the hole can be extracted to jets through the BZ process. The detailed physics is quite complicated, which has been extensively investigated in many previous works. For an extreme Kerr black hole, the maximal BZ power is

$$P_{\rm BZ}^{\rm max}\sim\frac{B_{\rm h}^2}{128}R_{\rm h}^2c, \quad (23)$$

where $B_{\rm h}$ is the strength of the field at the horizon, and $R_{\rm h}=GM_{\rm bh}/c^2$ for $a=1$ (MacDonald & Thorne 1982; Ghosh & Abramowicz 1997). This provides an upper limit on the jet power in GRBs.

3. RESULTS

In order to calculate the global structure of the NDAF as described in Section 2, we need to specify the boundary conditions at the outer radius $R_{\rm out}$. There are five parameters in our model calculations: viscosity parameter α, the mass accretion rate $\dot{M}$, the outer radius of the accretion disk $R_{\rm out}$, specific angular momentum of the gas in the NDAF j at $R_{\rm out}$, and the external magnetic field strength $B_{\rm ext}$.

A typical value of $\mathscr{P}_{\rm m}=1$ is adopted in this work (Parker 1979; Yousef et al. 2003; Lesur & Longaretti 2009; Fromang & Stone 2009; Guan & Gammie 2009). The black hole mass $M_{\rm bh}=3M_\odot$ is adopted in all the calculations. We use a fixed viscosity parameter: $\alpha=0.2$, in all the calculations, which is almost independent of the field advection, because the diffusion of magnetic field is proportional to the viscosity for a fixed Prandtl number. $j(R_{\rm out})=j_{\rm K}(R_{\rm out})$ is assumed at the outer radius of the NDAF, which affects little on the dynamics of the accretion flow. The global solution of a NDAF required to pass the sonic point smoothly is derived by tuning $j_{\rm in}$ carefully.

The NDAF is coupled with the magnetic field, i.e., the field configuration is determined by the NDAF structure, and the structure of the NDAF is also affected by the large scale field. We first calculate the global structure of the NDAF without magnetic field, and then the magnetic field is available based on the derived NDAF structure. The global solution of the NDAF is re-calculated based on this derived magnetic field. The global solutions converge usually after several iterations, because only the structure of the inner NDAF changes significantly due to the magnetic field.

As the pseudo-Newtonian potential is used in our calculations to simulate the general relativistic effect (see Section 2.1), the radial velocity of the NDAF approaches infinity at $R=R_{\rm S}$, which is unphysical. In the calculations of the global structure of the accretion flow, we define the radius of the black hole horizon as $R=R_{\rm h}$ where the radial velocity $v_R=c$. It is found that $R_{\rm h}\simeq 1.3-1.4\ R_{\rm S}$ depending on the values of mass accretion rate $\dot{M}$ and external field strength $B_{\rm ext}$ adopted in the calculations.

In Figure 1, we plot the large scale magnetic field configurations of NDAFs. The field is dragged inward efficiently by the gas in the NDAF. The structure of the NDAFs with different values of mass accretion rate $\dot{M}$ and external field strength $B_{\rm ext}$ is plotted in Figure 2. The radial velocity of the accretion flow with different disk parameters is quite similar. The R-dependent magnetic field strengths for the NDAFs with different values of the disk parameters are plotted in Figure 3. In Figure 4, we show how the magnetic field advection in the NDAF varies with the outer radius of the accretion flow. It is not surprising that the field strength at the region close to the horizon of the the black hole increases with the size of the disk if the values of all the other parameters are fixed.

For given external magnetic field strength, we calculate the structure and magnetic field of a NDAF with an outer radius $R_{\rm out}$ when the values of parameters, $\dot{M}$, and $B_{\rm ext}$ are specified. With the derived field strength at the black hole horizon, we estimate the maximal jet power extracted from an extreme Kerr black hole with Equation (23). The maximal Blandford-Znajek jet power as functions of the disk size is plotted in Figure 5 with different values of $\dot{M}$ and $B_{\rm ext}$. In Figure 6, we show how the structure of the NDAFs changes with the mass accretion rate $\dot{M}$ for given external magnetic field strength $B_{\rm ext}$. We find that the radial velocity of the accretion flow decreases near the black hole horizon if $\dot{M}$ is low, which implies the accretion flow is dynamically controlled/arrested by the magnetic field. The condition for arrested accretion flows is plotted in Figure 7.

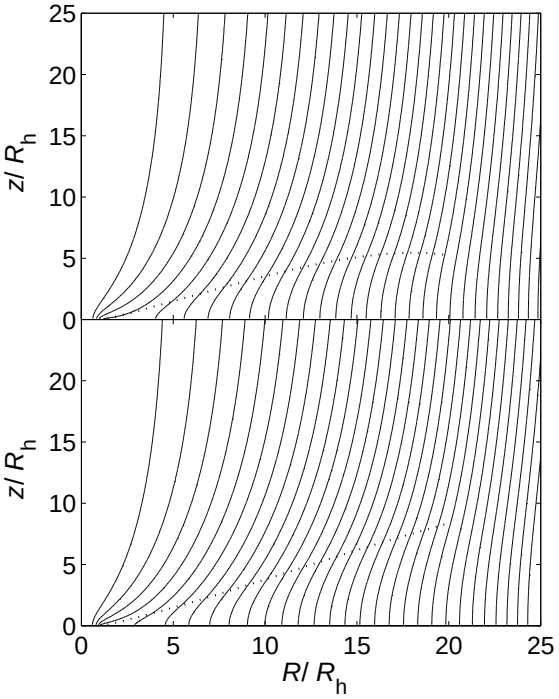

FIG. 1.— The large-scale poloidal magnetic field configurations of NDAFs. The outer radius of the disk is assumed to be $R_{\rm out} = 20R_{\rm h}$. The dotted line is the scale height of the NDAF. The magnetic field configuration plotted in the upper panel is calculated with $\dot{M} = 0.01M_{\odot}\ s^{-1}$ and $B_{\rm ext} = 10^{13}$ Gauss, while the lower panel is for $\dot{M} = 1M_{\odot}\ s^{-1}$ and $B_{\rm ext} = 10^{14}$ Gauss. Every magnetic field line corresponds to a certain value of the stream function $R\psi(R,z)$ with the lowest $[R\psi(R,z)]_{\rm min} = 0.1R_{\rm out}\psi_{\infty}(R_{\rm out},0)$ increasing by $\Delta R\psi(R,z) = 0.1R_{\rm out}\psi_{\infty}(R_{\rm out,0})$ per line, where $\psi_{\infty}(R_{\rm out}) = B_0R_{\rm out}/2$.

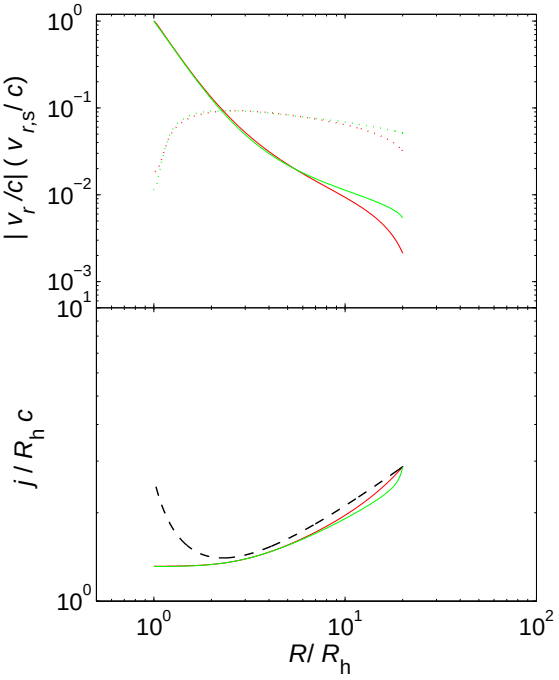

FIG. 2.— The structure of NDAFs with different values of disk parameters. The red lines indicate the results calculated with $\dot{M} = 0.01M_{\odot}\ s^{-1}$ and $B_{\rm ext} = 10^{13}$ Gauss, while the green lines are for the results with $\dot{M} = 1M_{\odot}\ s^{-1}$ and $B_{\rm ext} = 10^{14}$ Gauss. The radial velocity (solid lines) and sound speed (dotted lines) are plotted in the upper panel. In the lower panel, the specific angular momenta as functions of radius are plotted. The black dashed line represents the Keplerian specific angular momentum.

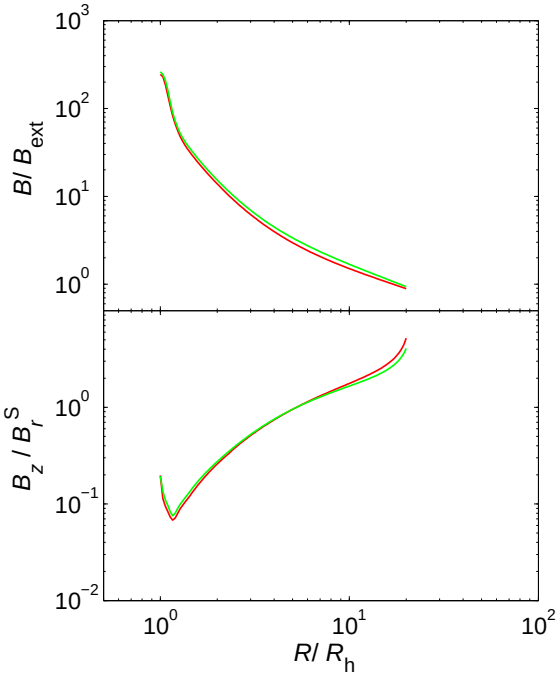

FIG. 3.— The magnetic field strengths as functions of radius for the NDAFs with different values of model parameters are plotted in the upper panel. The inclinations of the field lines at the disk surface are plotted in the lower panel. The red line indicates the result calculated with $\dot{M} = 0.01M_{\odot}\ s^{-1}$ and $B_{\rm ext} = 10^{13}$ Gauss, while the green line is for the result with $\dot{M} = 1M_{\odot}\ s^{-1}$ and $B_{\rm ext} = 10^{14}$ Gauss.

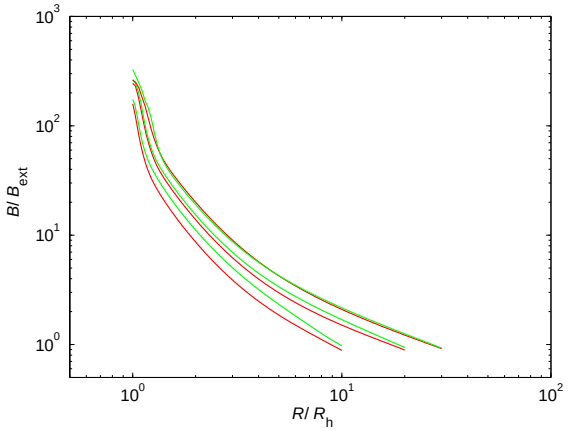

FIG. 4.— The magnetic field strengths as functions of radius for the NDAFs with different outer radii of NDAFs ($R_{\rm out} = 10R_{\rm h}$, $20R_{\rm h}$, and $30R_{\rm h}$). The red lines indicate the results calculated with $\dot{M} = 0.01M_{\odot}\ s^{-1}$ and $B_{\rm ext} = 10^{13}$ Gauss, while the green lines are for the results with $\dot{M} = 1M_{\odot}\ s^{-1}$ and $B_{\rm ext} = 10^{14}$ Gauss.

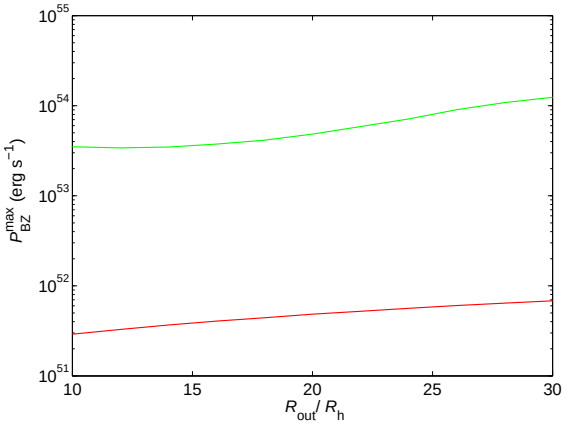

FIG. 5.— The maximal jet power can be extracted from extreme Kerr black holes surrounded by NDAFs. The red lines indicate the results calculated with $\dot{M} = 0.01 M_\odot\ s^{-1}$ and $B_{\rm ext} = 10^{13}$ Gauss, while the green lines are for the results with $\dot{M} = 1 M_\odot\ s^{-1}$ and $B_{\rm ext} = 10^{14}$ Gauss.

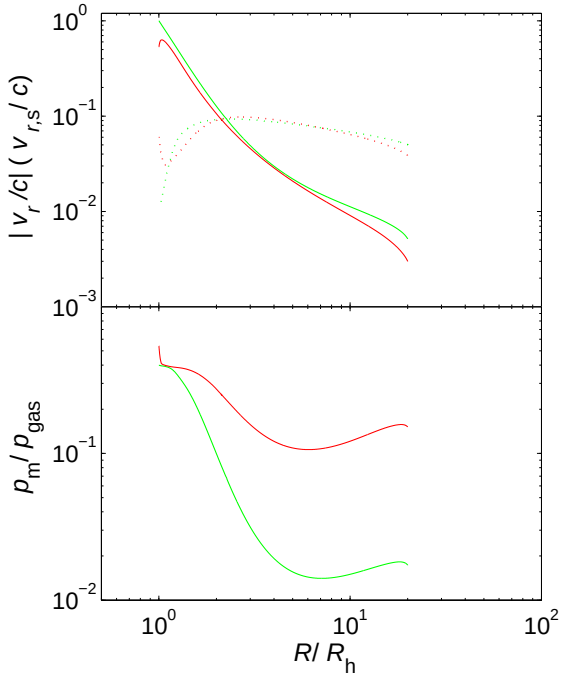

FIG. 6.— The structure and magnetic field strength of NDAFs. The strength of the external magnetic field $B_{\rm ext} = 10^{14}$ Gauss is adopted in the calculations. The red lines indicate the results calculated with $\dot{M} = 0.1 M_\odot\ s^{-1}$, while the green lines are for the results calculated with $\dot{M} = 1 M_\odot\ s^{-1}$. The radial velocity (solid lines) and sound speed (dotted lines) are plotted in the upper panel. In the lower panel, we plot the ratio of $p_{\rm m}/p_{\rm gas}$ as a function of radius.

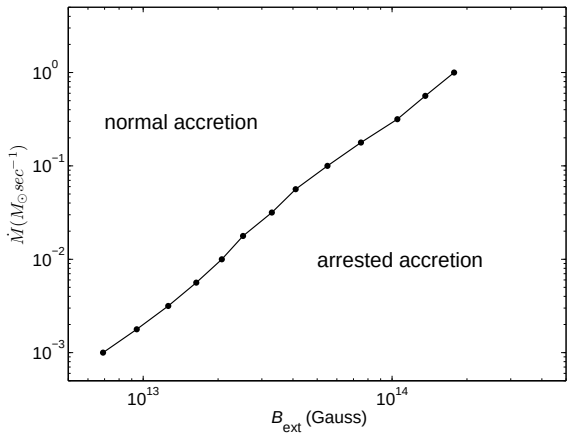

FIG. 7.— The critical mass accretion rate $\dot{M}$ for magnetically arrested accretion as a function of the external field strength $B_{\rm ext}$.

4. DISCUSSION

The external field can be dragged inward by the NDAF efficiently (see Figure 1). The magnetic field can hardly be advected by a geometrically thin standard accretion disks for a typical value of $\mathscr{P}_{\rm m} \sim 1$ (Lubow et al. 1994). The relative disk thickness H/R is large in the outer region of the NDAF (see Figure 1), which implies the field advection is more efficient in NDAF than the thin disk case considered in Lubow et al. (1994). The disk can be geometrically thin in the inner region of the NDAF, however, the gas falls almost freely onto the black hole horizon within the inner stable circular orbit of the black hole. Its radial velocity approaches the light speed at the black hole horizon, and therefore the external field is also dragged efficiently in the inner region of the NDAF towards the black hole. This is different from the calculations given in Lubow et al. (1994), in which the transonic characteristics of the accretion flow near the black hole have not been included. In their work, the gas in the standard thin disk is assumed to rotate at Keplerian velocity $v_{\rm K}$, and its radial velocity of the disk is approximated as $v_R = -3\nu/2R = -(3/2)(H/R)^2\alpha v_{\rm K}$, which is underestimated in the inner region of the disk.

For a given external magnetic field, the advection of the field in the NDAF can be calculated. We find that the field can be amplified more significantly for a NDAF with a larger size (a larger outer radius $R_{\rm out}$), due to the external field in a large area be captured by the accretion flow (see Figure 4, Narayan et al. 2003). The strength of the advected field at the black hole horizon is derived in our calculations, and then the maximal jet power is estimated. In principle, the calculations for the NDAF surrounding a rotating black hole should be carried out in the general relativistic frame (Xue et al. 2013), which is too complicated for our present investigation. The calculations based on the pseudo-Newtonian potential in this work show the main feature of the general relativistic accretion flow, i.e., the radial velocity approaches the light speed at the black hole horizon. We believe the estimates of the BZ jet power in this work based on the pseudo-Newtonian potential should be reliable at order of magnitude. In Figure 5, we show the maximal Blandford-Znajek jet power as functions of the disk size with different values of $\dot{M}$ and $B_{\rm ext}$. Our results show that the

maximal BZ jet power can be as $\sim 10^{53} - 10^{54}$ erg s^{-1} for an extreme Kerr black hole with $3M_\odot$, if an external magnetic field with 10^{14} Gauss is advected by the NDAF accreting at $\dot{M} = 1M_\odot$ s^{-1}, which is consistent with the typical field strength of a tidally disrupted magnetar (Liu et al. 2012). The tidal radius of a star disrupted by a black hole can be estimated by

$$R_{\rm T} \simeq 7.2 \left(\frac{M_{\rm bh}}{M_*}\right)^{1/3} R_*, \quad (24)$$

where M_* and R_* are the mass and radius of the star respectively (Rees 1988). For a typical magnetar with $M_* = 1.4M_\odot$ and $R_* = 10$ km captured by an extreme Kerr black hole with $M_{\rm bh} = 3M_\odot$, the tidal radius $R_{\rm T} \simeq 21R_{\rm h}$, which should be comparable with the outer radius of the NDAF.

An episodic soft gamma-ray tail is preferred to show in short-type GRBs, which are believed to be produced by mergers of compact stars (Hu et al. 2014). The steady configuration of the field dragged by the NDAF is achieved when the advection is balanced with magnetic diffusion (see Lubow et al. 1994, for the detailed discussion). We find that the accretion flow is arrested by the magnetic field close to the black hole horizon if the mass accretion rate $\dot{M}$ is low (see Figure 6). There is a critical mass accretion rate for a given external magnetic field, below which the accretion flow is arrested (see Figure 7). This implies that the accretion may be oscillating, because the balance between advection and diffusion is destroyed. When the accretion flow is arrested by the magnetic field, the accretion stops and the magnetic field decays due to magnetic diffusion. The accretion re-starts when the field becomes sufficiently weak, and the accretion flow may be arrested again if the advected field is strong enough. This will lead to episodic accretion, which is suggested to explain the observed oscillating soft extend emission in short-type GRBs (Proga & Zhang 2006; Liu et al. 2012).

As discussed above, the time interval of the episode accretion should be comparable with the magnetic field diffusion timescale. We can estimate the diffusion timescale of the field as (Lubow et al. 1994)

$$t_\eta \sim \frac{R^2}{\eta}\frac{H}{R}\frac{B_z}{B_r^{\rm S}} = \frac{1}{\alpha \mathscr{P}_{\rm m}\Omega_{\rm K}}\frac{B_z}{B_r^{\rm S}}\left(\frac{H}{R}\right)^{-1}$$

$$= 4.92\times10^{-6}\frac{M}{M_\odot}\frac{B_z}{B_r^{\rm S}}\left(\frac{R}{R_{\rm h}}\right)^{3/2}\left(\frac{H}{R}\right)^{-1}\alpha^{-1}\mathscr{P}_{\rm m}^{-1}\ {\rm s}. \quad (25)$$

The poloidal magnetic field of the NDAF is maintained by the azimuthal currents in the whole disk, which is a global problem, and therefore we adopt typical values of the quantities at the outer radius of the NDAF in estimating the diffusion timescale of the field threading the disk. If we adopt $H/R = 0.2$, and $B_z/B_r^{\rm S} = 5$ at $R_{\rm out}$ (see Figures 1 and 3), the diffusion timescale $t_\eta \sim 0.2$ seconds, for the typical values of the parameters, $\mathscr{P}_{\rm m} = 1$, $\alpha = 0.2$, and $R = 20R_{\rm h}$. The size of the disk may expand with time due to the angular momentum transfer in the disk (see Figure 5.1 in Frank et al. 2002), which implies that the radius of the arrested NDAF at late stage may be larger than the tidal radius $R_{\rm T}$. Thus, the interval timescale of the episodic accretion could be longer than the estimate, which is roughly consistent with the observed oscillation in the soft extend emission of short-type GRBs (see Figure 2 in Liu et al. 2012, for the observed light curves of some typical GRBs).

We thank the referee for his/her helpful comments/suggestions, and Dong Lai for discussion. This work is supported by the NSFC (grants 11173043, 11121062, 11233006, and 11025313), the CAS/SAFEA International Partnership Program for Creative Research Teams (KJCX2-YW-T23), the Strategic Priority Research Program of the Chinese Academy of Sciences (XDB09000000). E. W. Liang acknowledges support by the National Basic Research Program (973 Programme) of China (Grant 2014CB845800) and the Guangxi Science Foundation (2013GXNSFFA019001).

REFERENCES

Abdo, A. A., Ackermann, M., Arimoto, M., et al. 2009, Science, 323, 1688
Balbus, S. A., & Hawley, J. F. 1991, ApJ, 376, 214
Balbus, S. A., & Hawley, J. F. 1998, Reviews of Modern Physics, 70, 1
Barkov, M. V., & Komissarov, S. S. 2010, MNRAS, 401, 1644
Beckwith, K., Hawley, J. F., & Krolik, J. H. 2009, ApJ, 707, 428
Blandford, R. D., & Znajek, R. L. 1977, MNRAS, 179, 433
Cao, X. 2011, ApJ, 737, 94
Cao, X., & Spruit, H. C. 2002, A&A, 385, 289
Cao, X., & Spruit, H. C. 2013, ApJ, 765, 149
Chen, W.-X., & Beloborodov, A. M. 2007, ApJ, 657, 383
Daigne, F., & Mochkovitch, R. 2002, MNRAS, 336, 1271
Deaton, M. B., Duez, M. D., Foucart, F., et al. 2013, ApJ, 776, 47
Di Matteo, T., Perna, R., & Narayan, R. 2002, ApJ, 579, 706
Eichler, D., Livio, M., Piran, T., & Schramm, D. N. 1989, Nature, 340, 126
Etienne, Z. B., Liu, Y. T., Paschalidis, V., & Shapiro, S. L. 2012, Phys. Rev. D, 85, 064029
Foucart, F., Deaton, M. B., Duez, M. D., et al. 2013, Phys. Rev. D, 87, 084006
Frank, J., King, A., & Raine, D. J. 2002, Accretion Power in Astrophysics, by Juhan Frank and Andrew King and Derek Raine, pp. 398. ISBN 0521620538. Cambridge, UK: Cambridge University Press, February 2002
Fromang, S., & Stone, J. M. 2009, A&A, 507, 19
Ghosh, P., & Abramowicz, M. A. 1997, MNRAS, 292, 887
Gu, W.-M., Liu, T., & Lu, J.-F. 2006, ApJ, 643, L87
Guan, X., & Gammie, C. F. 2009, ApJ, 697, 1901
Guilet, J., & Ogilvie, G. I. 2012, MNRAS, 424, 2097
Guilet, J., & Ogilvie, G. I. 2013, MNRAS, 430, 822
Hu, Y. D., Liang, E. W., Xi, S. Q., et al. 2014, ApJ, submitted
Janiuk, A., Moderski, R., & Proga, D. 2008, ApJ, 687, 433
Kawanaka, N., & Mineshige, S. 2007, ApJ, 662, 1156
Kawanaka, N., Piran, T., & Krolik, J. H. 2013, ApJ, 766, 31
Kippenhahn, R., & Schlüter, A. 1957, Z. Astrophys., 43, 36
Kohri, K., & Mineshige, S. 2002, ApJ, 577, 311
Kohri, K., Narayan, R., & Piran, T. 2005, ApJ, 629, 341
Lee, W. H., Ramirez-Ruiz, E., & Page, D. 2005, ApJ, 632, 421
Lei, W. H., Wang, D. X., Zhang, L., et al. 2009, ApJ, 700, 1970
Lesur, G., & Longaretti, P.-Y. 2009, A&A, 504, 309
Li, L.-X. 2000, ApJ, 533, L115
Liu, T., Gu, W.-M., Xue, L., & Lu, J.-F. 2007, ApJ, 661, 1025
Liu, T., Liang, E.-W., Gu, W.-M., et al. 2012, ApJ, 760, 63

Lovelace, R. V. E., Rothstein, D. M., & Bisnovatyi-Kogan, G. S. 2009, ApJ, 701, 885
Lubow, S. H., Papaloizou, J. C. B., & Pringle, J. E. 1994, MNRAS, 267, 235
MacDonald, D., & Thorne, K. S. 1982, MNRAS, 198, 345
McKinney, J. C. 2005, ApJ, 630, L5
Narayan, R., Igumenshchev, I. V., & Abramowicz, M. A. 2003, PASJ, 55, L69
Narayan, R., Piran, T., & Kumar, P. 2001, ApJ, 557, 949
Narayan, R., & Yi, I. 1994, ApJ, 428, L13
Paczynski, B. 1998, ApJ, 494, L45
Paczyński, B., & Wiita, P. J. 1980, A&A, 88, 23
Pan, Z., & Yuan, Y.-F. 2012, ApJ, 759, 82
Parker, E. N. 1979, in Chapter 17, Cosmical Magnetic Fields (Oxford:Clarendon Press)
Piran, T. 2004, Reviews of Modern Physics, 76, 1143
Popham, R., Woosley, S. E., & Fryer, C. 1999, ApJ, 518, 356
Proga, D., & Zhang, B. 2006, MNRAS, 370, L61
Rees, M. J. 1988, Nature, 333, 523
Ruffert, M., & Janka, H.-T. 1998, A&A, 338, 535
Wang, D. X., Xiao, K., & Lei, W. H. 2002, MNRAS, 335, 655
Woosley, S. E. 1993, ApJ, 405, 273
Woosley, S. E., & Bloom, J. S. 2006, ARA&A, 44, 507
Xue, L., Liu, T., Gu, W.-M., & Lu, J.-F. 2013, ApJS, 207, 23
Yousef, T. A., Brandenburg, A., Rüdiger, G. 2003, A&A, 411, 321
Yuan, F., & Zhang, B. 2012, ApJ, 757, 56
Zhang, B., & Mészáros, P. 2002, ApJ, 581, 1236
Zhang, B., & Mészáros, P. 2004, International Journal of Modern Physics A, 19, 2385
Zhang, B., & Pe'er, A. 2009, ApJ, 700, L65
Zhang, B., & Yan, H. 2011, ApJ, 726, 90
Zhang, B.-B., Zhang, B., Liang, E.-W., et al. 2011, ApJ, 730, 141